

# Amplified detection of DNA by an analyte-induced Y-shaped junction probe assembly followed with a nicking endonuclease-mediated autocatalytic recycling process†

Cite this: *Chem. Commun.*, 2013, **49**, 7947

Received 11th July 2013,  
Accepted 18th July 2013

DOI: 10.1039/c3cc45211e

[www.rsc.org/chemcomm](http://www.rsc.org/chemcomm)

Shufeng Liu,<sup>a</sup> Chengxin Zhang,<sup>b</sup> Jingjing Ming,<sup>b</sup> Chunfeng Wang,<sup>b</sup> Tao Liu<sup>b</sup> and Feng Li<sup>\*a</sup>

**A simple, isothermal and autocatalytic system for the amplified detection of DNA was ingeniously designed based on target-triggered Y-shaped junction probe assembly, followed with a nicking endonuclease-mediated cascade recycling process. A superior detection limit of 0.1 pM towards the target DNA with an excellent selectivity could be achieved.**

In order to satisfy the requirements for profiling the low abundance of target DNA,<sup>1</sup> the DNA-based nanomachine has become an attractive tool with great potential to replace the polymerase chain reaction (PCR), due to its easy operation, isothermal reaction, and high sensitivity.<sup>2</sup> Its operation is generally involved with the target recycling *via* nucleases, accompanied with the autonomous generation of new target analogues. For example, the autonomous replication–scission–displacement process based on nicking endonuclease and polymerase was reported as an effective amplified system for the detection of nucleic acids.<sup>3</sup> More recently, a one-pot hairpin-mediated quadratic enzymatic amplification strategy has been proposed for nucleic acid detection based on the combination of nicking endonuclease, exonuclease and polymerase.<sup>4</sup> However, the employment of multiple nucleases increases the assay cost, and also may cause undetermined effects or even a false-positive signal in the target detection. The Exonuclease III (Exo III)-mediated autocatalytic recycling amplification has also been utilized for the sensitive detection of DNA,<sup>5</sup> yet the requirement of relatively complex design procedures limits its wide application. Recently, Willner *et al.* reported an isothermal, autocatalytic strategy for DNA detection using a Mg<sup>2+</sup>-dependent DNzyme as a biocatalyst.<sup>6</sup> Even though such a system does not require protein-based enzymes, the ribonucleotide-containing substrate for the DNzyme is often confronted with a higher

synthesis cost and is susceptible to ribonuclease and chemical degradation. In this context, the development of a simple, isothermal, sensitive and autocatalytic amplification system is highly desirable for applications in DNA diagnostics.

Compared with Exo III,<sup>7</sup> nicking endonuclease is especially attractive for the biomolecule's detection, owing to its strong recognition for DNA sequences.<sup>8</sup> However, the major limitation for the use of nicking endonuclease lies in the requirement for the target of interest to contain a specific sequence. Alternatively, a Y-shaped junction probe based detection platform has been recently designed for target DNA detection, based on a so-called “template enhanced hybridization process”, and can effectively obviate this issue.<sup>9</sup> Moreover, a target-complementary arched structure is developed for signal amplification based on nicking endonuclease mediated-assistant DNA recycling and a molecular beacon (MB).<sup>10</sup> In these designs, only conventional nicking endonuclease-mediated signal amplification is utilized for target detection, and its sensitivity needs to be further improved.

Herein, a simple, isothermal and autocatalytic system for the amplified detection of a target DNA was proposed for the first time based on an analyte-induced Y-shaped junction probe assembly followed with a nicking endonuclease-mediated cascade recycling process. The principle for the designed autocatalytic sensing system is illustrated in Fig. 1. The system includes a hairpin-structured molecular beacon (MB), which is modified at its 3' and 5' ends with a quencher and a fluorophore, respectively, and two subunits, 1 and 2. Subunit 1 forms a hairpin structure that includes the base sequence complementary to the analyte in the loop region and the stem domain (red region). The subunits 1 and 2 contain the base sequence that can respectively hybridize with the hairpin-structured MB in the domains I and II, as well as nucleic acid tethers III and IV, which exhibit mutual base complementarities. As the domain III of subunit 1 is blocked by the hairpin stem region, the domain IV of subunit 2 can not hybridize with the domain III of subunit 1, thus the Y-shaped junction structure can not be formed and the MB can not be opened for further cleavage by the nicking endonuclease. Upon interaction of the subunit 1 with the target DNA, the hairpin

<sup>a</sup> College of Chemistry and Pharmaceutical Sciences, Qingdao Agricultural University, 700 Changcheng Road, Qingdao 266109, China.

E-mail: lifeng@qust.edu.cn

<sup>b</sup> College of Chemistry and Molecular Engineering, Qingdao University of Science and Technology, Qingdao 266042, China

† Electronic supplementary information (ESI) available: Experimental details and additional information. See DOI: 10.1039/c3cc45211e

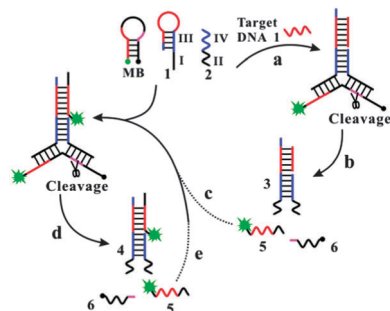


**Fig. 1** Schematic illustration of the analyte-induced Y-shaped junction probe assembly and the sensing process: (a) target recognition and assembly of the Y-shaped junction probe; (b) cleavage of the substrate MB and release of the activator unit 5; (c)–(e) autocatalytic catabolic generation cycle triggered by the activator unit-induced assembly of the Y-shaped junction probe.

structure of subunit 1 is opened and exposes domain III, thereby giving rise to the assembly of the subunits 1 and 2 into structure 3 through the hybridization of domains III and IV. The synergistic binding of the MB to the structure 3 results in the formation of a stable Y-shaped junction structure. In this structure, the hybridized double-stranded DNA between the subunit 2 and MB provides the specific nucleotide sequence for recognition and cleavage by the nicking endonuclease Nt.BbvCI. The lack of sufficient base-pairing stability for the cleaved MB leads to the release of the fragments 5 and 6 from structure 3, and allows the continuous scission of the MB. The designed MB also contains the sequence of the target DNA, but the stable hairpin structure preserves this sequence in a sequestered structure, thus prohibiting the activation in the absence of the target DNA. The released fluorophore-labeled nucleic acid fragment 5 generates a high fluorescence intensity for the sensing of the target DNA. The fragment 5 also includes the base sequence of the target DNA and can be used as a new activator unit to open subunit 1. This process leads to the enhanced formation of structure 4 and the increased cleavage of MB, with the concomitant generation of a fluorescent signal of higher intensity. Thus, in the presence of the target DNA, the autonomous, autocatalytic accumulation of the analyte sequence is activated, which leads to the effective generation of structure 4 for the distinctly amplified signal.

The feasibility of the proposed autocatalytic sensing system for target DNA detection was first verified and is shown in Fig. 2. Only a small background fluorescence of the MB can be observed in the absence of Nt.BbvCI and target DNA (Fig. 2a). The addition of Nt.BbvCI in the absence of target DNA can result in an increased background fluorescence (Fig. 2b), which can be attributed to the fact that the Nt.BbvCI cleaves some of the MB that may be partially hybridized to the subunit 2. Fortunately, the target-induced signal enhancement is much higher than the background signal, ensuring high sensitivity for the detection of the target DNA. As shown in Fig. 2d, by introducing nicking endonuclease amplification, we observed an approximately 4.5-fold signal increase upon the addition of 1 nM target DNA. The corresponding signal enhancement in the absence of nicking endonuclease was only about 83% (Fig. 2c). Control experiments with substitution of the target DNA by a non-complementary target showed almost no fluorescence

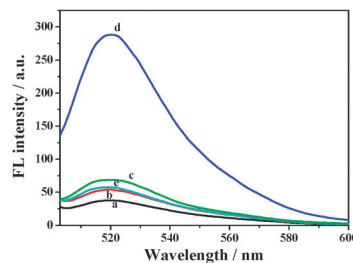


**Fig. 2** Fluorescence spectra of the sensing system of 300  $\mu\text{L}$   $1 \times$  NEB buffer 4 (20 mM Tris-Ac, 10 mM  $\text{Mg}(\text{Ac})_2$ , 50 mM KAc, 1 mM DTT, pH 7.9), containing 50 nM MB and 50 nM of subunits 1 and 2 after incubation for 30 min at 37  $^\circ\text{C}$ , with (a) no Nt.BbvCI, no target; (b) 0.04  $\text{U } \mu\text{L}^{-1}$  Nt.BbvCI, no target; (c) no Nt.BbvCI, 1 nM target; (d) 0.04  $\text{U } \mu\text{L}^{-1}$  Nt.BbvCI, 1 nM target; (e) 0.04  $\text{U } \mu\text{L}^{-1}$  Nt.BbvCI, 1 nM non-complementary target.

change compared with that in the absence of target DNA (Fig. 2e). These results fully indicate that our developed sensing system can feasibly provide an amplified signal for target detection.

In order to achieve the best sensing performance, the sequences of the subunit 1 and MB, fluorescence response time and concentrations of both Nt.BbvCI and MB were optimized. The subunit 1 containing a stem length of 8 base pairs could give the best analytical results compared with the subunit 1 containing 6, 7, and 9 base pairs in the stem region (Fig. S1, ESI $^\dagger$ ). The MB that provides the readout signal includes the target DNA sequence as a built-in component, and this sequence should be fully hybridized and sequestered in the stable hairpin structure of MB to eliminate the opening of the hairpin subunit 1 in the absence of target DNA. Our experimental results showed that a MB containing a stem of six base pairs could provide a better sensing performance than the MBs with a stem of five and seven base pairs (Fig. S2, ESI $^\dagger$ ). The fluorescence response time for target DNA detection was optimized at 30 min (Fig. S3, ESI $^\dagger$ ). The experimental results also showed that a concentration of 0.04  $\text{U } \mu\text{L}^{-1}$  of endonuclease and 50 nM MB can provide the optimal sensing results (Fig. S4 and S5, ESI $^\dagger$ ).

To further prove the signal amplification effect of the autocatalytic recycling strategy, another hairpin MB, MB 2, was also designed as a substitute MB for comparison. The only difference of the MB 2 with the advised MB is that the sequence of the target DNA preserved in the MB is substituted by a non-target sequence. That is, in the presence of the target DNA, the synergistic binding of the subunit 1 and 2 to the MB 2 results also in the formation of a stable Y-shaped junction structure for further recognition and cleavage by nicking endonuclease, but the released fluorophore-labeled fragment after cleavage can not act as a new activator unit to open subunit 1. Thus, no new target analogues are generated in this case, and only the formed DNA hybrid 3 can be recycled to trigger the successive cleavage process. It could be denoted as a typical nicking endonuclease-mediated recycling strategy. This typical recycling strategy only showed a detection limit of about 20 pM for target DNA (Fig. S6, ESI $^\dagger$ ). In contrast, the fluorescence response to the target DNA by the autocatalytic recycling strategy at the same concentration was significantly higher than that by the typical recycling strategy. Also, the developed autocatalytic recycling strategy

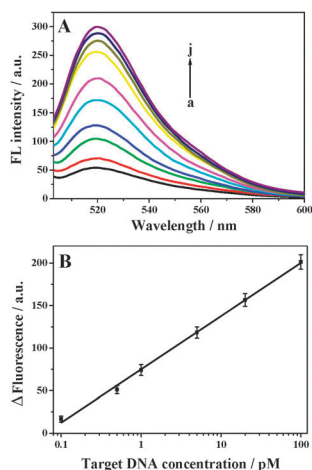


**Fig. 3** (A) Fluorescence spectra of the autocatalytic nucleic acid sensing in the presence of different target DNA concentrations: (a) 0 pM, (b) 0.1 pM, (c) 0.5 pM, (d) 1 pM, (e) 5 pM, (f) 20 pM, (g) 100 pM, (h) 500 pM, (i) 1 nM and (j) 2 nM. (B) The linear relationship between the fluorescence signal change and target concentration from 0.1 pM to 100 pM.  $\Delta$ Fluorescence was calculated by  $F - F_0$ , where  $F$  and  $F_0$  are the fluorescence intensities observed in the presence and absence of target DNA, respectively. The error bars represent the standard deviation of three measurements.

can achieve a more rapid fluorescence response before reaching equilibrium, compared with that of the typical recycling strategy (Fig. S3, ESI<sup>†</sup>), indicating that the autocatalytic recycling process indeed occurs.

Fig. 3A shows the fluorescence-emission spectra of the autocatalytic sensing system upon the addition of target DNA at different concentrations. As the concentration of target DNA increases, the fluorescence intensity generated by the sensing system also increases. Under the optimal conditions, the fluorescence intensity change showed a good linear correlation with the logarithmic value of the target DNA concentration ranging from 0.1 pM to 100 pM (Fig. 3B). A directly measured detection limit towards the target DNA is obtained to be as low as 0.1 pM, which is distinctly lower than that of the Y-shaped junction structure (5 pM),<sup>9a</sup> conventional nicking endonuclease signal amplification (20 pM)<sup>11</sup> and Mg<sup>2+</sup>-dependent DNAzyme mediated autocatalytic signal amplification (1 pM)<sup>6</sup> with fluorescence measurements.

The proposed sensing system also shows a remarkably high sequence specificity for DNA detection (Fig. S7, ESI<sup>†</sup>). An excellent discrimination ability of the proposed strategy against a single-base mismatch could be observed.<sup>12</sup> We further challenged the detection towards target DNA spiked in a relatively complex biological matrix (1:10 dilution of human serum). Comparable responses were obtained for the detection of target DNA in both buffer and real samples (Fig. S8, ESI<sup>†</sup>), indicating the potential for real analytical applications.

Furthermore, the proposed autocatalytic sensing strategy can also be developed as a versatile approach for the sensing

of any DNA sequences (Fig. S9, ESI<sup>†</sup>). The analytical process includes a sensing module (non-autocatalytic process) that initiates the autocatalytic module. The only added component is the subunit 7, which contains the appropriate loop domain for the respective target analyte in the hairpin. The stem region in hairpin 7 is identical to the stem in subunit 1. The assembly of the Y-shaped junction structure upon sensing of the new target DNA results in the cleavage of the MB. The released fluorophore-labeled fragment 5 allows the opening of the hairpin-blocking subunit 1, thus activating the autocatalytic cycle. With the concentration increase of the target DNA, the fluorescence response is intensified. Also, a low background signal is observed in the absence of the target DNA.

In conclusion, an autocatalytic nucleic acid sensing system was fully developed based on an analyte-induced Y-shaped junction structure assembly followed with a nicking endonuclease-mediated recycling process. It is a promising approach to develop the nuclease-based autocatalytic sensing of analytes.

This work was funded by the National Natural Science Foundation of China (No. 21005043, 21175076), the Basic Research Program of Qingdao (No. 13-1-4-214-jch) and the Science Foundation of China Postdoctor (No. 2012M511537).

## Notes and references

- (a) A. Sassolas, B. D. Leca-Bouvier and L. J. Blum, *Chem. Rev.*, 2008, **108**, 109; (b) N. K. Navani and Y. Li, *Curr. Opin. Chem. Biol.*, 2006, **10**, 272; (c) A. R. Connolly and M. Trau, *Nat. Protoc.*, 2011, **6**, 772.
- (a) W. Xu, X. Xue, T. Li, H. Zeng and X. Liu, *Angew. Chem., Int. Ed.*, 2009, **48**, 6849; (b) J. Ren, J. Wang, L. Han, E. Wang and J. Wang, *Chem. Commun.*, 2011, **47**, 10563; (c) Y. Weizmann, Z. Cheglakov and I. Willner, *J. Am. Chem. Soc.*, 2008, **130**, 17224; (d) R. Orbach, L. Mostinski, F. Wang and I. Willner, *Chem.-Eur. J.*, 2012, **18**, 14689.
- (a) Q. Guo, X. Yang, K. Wang, W. Tan, W. Li, H. Tang and H. Li, *Nucleic Acids Res.*, 2009, **37**, e20; (b) Y. Weizmann, M. K. Beissenhirtz, Z. Cheglakov, R. Nowarski, M. Kotler and I. Willner, *Angew. Chem., Int. Ed.*, 2006, **45**, 7384; (c) C. Y. Zhang and G. L. Wang, *Anal. Chem.*, 2012, **84**, 7037; (d) H. Jia, Z. Li, C. Liu and Y. Cheng, *Angew. Chem., Int. Ed.*, 2010, **49**, 5498.
- R. Duan, X. Zuo, S. Wang, X. Quan, D. Chen, Z. Chen, L. Jiang, C. Fan and F. Xia, *J. Am. Chem. Soc.*, 2013, **135**, 4604.
- (a) S. Liu, C. Zhang, C. Wang and B. Tang, *Anal. Chem.*, 2013, **85**, 2282; (b) S. Bi, L. Li and Y. Cui, *Chem. Commun.*, 2012, **48**, 1018.
- F. Wang, J. Elbaz, C. Teller and I. Willner, *Angew. Chem., Int. Ed.*, 2011, **50**, 295.
- X. Zuo, F. Xia, Y. Xiao and K. W. Plaxco, *J. Am. Chem. Soc.*, 2010, **132**, 1816.
- (a) J. J. Li, Y. Z. Chu, B. Y. H. Lee and X. L. S. Xie, *Nucleic Acids Res.*, 2008, **36**, e36; (b) S. Bi, J. Zhang and S. Zhang, *Chem. Commun.*, 2010, **46**, 5509.
- (a) R. M. Kong, X. B. Zhang, L. L. Zhang, Y. Huang, D. Q. Lu, W. Tan, G. L. Shen and R. Q. Yu, *Anal. Chem.*, 2011, **83**, 14; (b) Y. Li, Y. T. Hong and D. Luo, *Nat. Biotechnol.*, 2005, **23**, 885; (c) S. Nakayama, L. Yan and H. O. Sintim, *J. Am. Chem. Soc.*, 2008, **130**, 12560.
- F. Gao, J. Lei and H. Ju, *Chem. Commun.*, 2013, **49**, 4006.
- T. Kiesling, K. Cox, E. A. Davidson, K. Dretchen, G. Grater, S. Hibbard, R. S. Lasken, J. Leshin, E. Skowronski and M. Danielsen, *Nucleic Acids Res.*, 2007, **35**, e117.
- (a) S. Tyagi and F. R. Kramer, *Nat. Biotechnol.*, 1996, **14**, 303; (b) G. Bonnet, S. Tyagi, A. Libchaber and F. R. Kramer, *Proc. Natl. Acad. Sci. U. S. A.*, 1999, **96**, 6171.